Chapter 8

Plasma Control System

Valerij A. Belyakov, Andrej A. Kavin
JSC D.V. Efremov Scientific Research Institute of Electrophysical Apparatus, Saint Petersburg, Russia

Chapter Outline

8.1 INTRODUCTION

This chapter deals with the optimisation design of the plasma position, shape and current control system at different phases of discharge. It presents derivation of the plasma linear models and feedback control algorithms. The methods of the nonlinear simulation of plasma control system with the free-boundary codes and features of the simulation of the initial phase of discharge are described. The application scope of such models is estimated.

The methods discussed here allow for the evaluation of passive plasma stabilisation effectiveness, give the possibilities for optimising tokamak design and synthesis of the controllers and specify requirements for the poloidal field coils' power supply systems.

Fundamentals of Magnetic Thermonuclear Reactor Design. http://dx.doi.org/10.1016/B978-0-08-102470-6.00008-1
Copyright © 2018 Elsevier Ltd. All rights reserved.

The methods of correction of the magnetic error fields due to inaccuracies of tokamak manufacturing and assembly are considered. The problems of the plasma position and shape reconstruction based on magnetic field measurements are discussed.

8.2 SCOPE OF THE CONTROL SYSTEM DESIGN PROBLEM

The fusion reactor's operation cycle includes several stages. Actually, it consists of a series of electro-physical and electro-technical operations, which are characterised by stationary, variable and alternating electromagnetic fields. The tokamak's typical operation cycle includes the following stages and plasma processes:

- initial magnetisation of the poloidal field coils
- D–T gas breakdown in the vacuum vessel and plasma initiation
- plasma current ramp-up
- formation of a divertor configuration
- auxiliary heating of plasma
- plasma burn phase
- plasma current termination and quench of fusion.

We remember that a stationary toroidal field must be provided before the beginning of the operation cycle.

Topologically, the tokamak plasma magnetic field is a set of closed magnetic flux surfaces, placed one inside another. It is characterised by the plasma minor radius a_p and major radius R_p. For an elongated plasma, there are the elongation k_p and triangularity δ_p coefficients. Such magnetic flux surfaces can be expressed as a parametric function:

$$r = R_p + a_p \cos(\theta + \delta_p \sin\theta),$$
$$z = a_p k_p \sin\theta,$$

where θ is the poloidal angle.

Last closed magnetic flux surfaces are often described using geometric parameters a_{95}, R_{95}, k_{95} and δ_{95}, measured/computed upon an assumption that the magnetic flux surface has 95% of the total poloidal magnetic flux. This is especially convenient when dealing with plasmas in divertor configurations, where the separatrix topologically separates magnetic field lines closed within the plasma region from those closed around the poloidal field coils.

The synthesis of the plasma control system leads to an optimisation solution of a complex of interconnected engineering problems, such as the following:

- Developing programmed scenarios for different stages of the plasma discharge.

- Control of plasma current and plasma integral parameters (R_p, a_p, k_p, and δ_p), plasma magnetic configuration (e.g. gaps between the first wall and the plasma boundary), and magnetic configuration in the divertor region (including the *X*-point position, the separatrix branches trajectory in the divertor channels, and the location of strike points on divertor plates). This also includes the correction of error fields disturbing the magnetic axis symmetry, and the corpuscular and magnetic diagnostics of the plasma column position and shape.
- Control of divertor plasmas (density, fusion power, impurity content and radiation power, gas puffing to the divertor chamber, etc.).
- Optimisation of the magnet configuration to improve the divertor performance.
- Fast plasma termination by an impurity/hydrogen injection.

This list of engineering problems reflects their phenomenological differences and hierarchy of concepts. Developing of plasma scenarios is the highest priority problem. Next comes control of the magnet configuration, because it has to be adapted to a scenario algorithm. For the control of plasma configuration, the magnetic measurements are sufficient without kinetic plasma parameters. As to the quench of fusion, it is quite a stand-alone problem.

The discussed control systems have certain parametric and model uncertainties, complicating their design and optimisation, namely, the 'dynamic instability' of the plasma itself, the non-linearity of plasma processes and a host of other factors to be accounted for. The latter include the following:

- Fast changes in the current (I_p) and the plasma major radius (R_p), internal inductance (l_i), and poloidal beta (β_p).
- Currents induced in the complex metallic structures surrounding the plasma.
- Electromagnetic coupling between the plasma column, coils and induced currents at the high power (tens of megawatt) required for the plasma control.

Hence, an optimisation design of control systems with feedback loops (also called closed-loop control systems, CLCSs) is only possible using numerical simulation that describes plasma behaviour and response to external perturbations with the control actions.

8.3 BASIC DESIGN METHODOLOGY

Plasma control systems are often designed using the following sequence of logical and mathematical procedures:

- Providing a set of plasma basic static equilibrium states describing its evolution for the given variations of the plasma physical parameters. The latter, generally, are integral parameters I_p, R_p, a_p, k_p, l_i, β_p, and ψ_{res} (ψ_{res} are magnetic flux losses due to plasma ohmic resistance).

- Developing linear models characterizing the dynamics of plasma position, shape and current near a basic equilibrium.
- Synthesis of the plasma feedback control algorithms (selecting controllers based on the linear models).
- Nonlinear modelling of plasma discharge scenarios, accounting for the preprogrammed control and the synthesised feedback controllers. This analysis is performed using codes describing the plasma parameter behaviour as comprehensively as possible.
- Correction of the preprogrammed/feedback control where necessary.

A generally accepted method for calculating each of the basic equilibriums is to find poloidal coil currents according to the given resistive losses at the variations of the integral parameters I_p, l_i, R_p and the plasma shape. The resistive losses are estimated (based either on physical scaling or phenomenological concepts). Simultaneously the poloidal coil voltages are determined for the assessment of the requirements to the power supply system. Currents induced in passive structures are neglected; therefore, every basic equilibrium is calculated independently. The results of these calculations determine the evolution of plasma parameters and current in the poloidal coils which, along with the power supply system, is to be provided by the control system under design.

An alternative approach to calculate the basic equilibriums is to use profiles of the plasma poloidal current, stability margin q and plasma pressure profiles (derived experimentally or theoretically) as input data, instead of the integral I_p, l_i, and R_p parameters. This method allows poloidal coil currents to be estimated more reliably.

Numerical modelling is a centrepiece of the control system design. Linear models are commonly used, as they enable the following:

- Evaluation of a passive plasma stabilisation effectiveness and optimisation of conductive elements' geometry, which is especially important for vertically unstable plasmas.
- Determination of the requirements for good performance of poloidal field coil power supplies in terms of power and operating speed.
- Synthesising of controllers providing feedback stabilisation of a plasma column. It should be noted that the modern theory of controller synthesis has high development for the linear control objects.

Engineering practices have proved the adequacy of the linear numerical models for the development of CLCSs. Such models have been extensively used, among other things, in ITER design, assisting engineers in optimising the geometry of the vacuum vessel and the in-vessel components to provide the acceptable timescale of the control processes for plasmas with extreme elongation. They also laid the groundwork for the design of the interconnected plasma control and PFC power supply systems.

8.4 MATHEMATICAL MODELLING OF ELECTROMAGNETIC PROCESSES

8.4.1 Derivation of Linear Models

We assume that plasma column displacements are small and axisymmetric and ignore plasma electrical resistance and viscosity. In other words, we confine ourselves to considering ideal, non-inertial plasma in frame of the classical magnetohydrodynamic(MHD) theory. We also assume that plasma is stable on an Alfvén timescale and that our linear model describes only the processes on the timescale comparable with the time constants of the conducting structures. Our aim is to obtain matrixes of linear equations (MLE) describing the behaviour of plasma and currents in surrounding conducting structures under equilibrium conditions. In a general case, the evolution of interest is described by a system of nonlinear partial differential equations, namely, the Grad–Shafranov equation for equilibrium and electro-technical equations for plasma and circuit currents. To solve this, we use numerical methods. The model of the response of the free boundary equilibrium plasma on the disturbance of the currents in the surrounding conductors is used for the linearisation. Here, we follow the approaches described in Refs [1, 2].

To linearise any equations, we have to define a set of states, or variables that determine the linear model dynamics. Plasma position and shape evolution depends on currents in poloidal field coils and passive circuits.

It is therefore natural to use deviations of those currents relative to initial (base) values as linear model states:

$$\delta I(t) = I(t) - I_0, \tag{8.1}$$

where $I(t)$ denotes currents at time t, and I_0 refers to currents for the initial (base) configuration ($t = 0$).

The dynamics of circuit currents (states) is expressed by electro-technical equations of the form

$$\frac{d\Psi}{dt} + RI = U, \tag{8.2}$$

where ψ is the poloidal flux vector averaged over the circuit cross-section, R is the matrix of circuit resistances, and U is the vector of external voltages applied to the circuits. In a linear case, vector ψ can be expressed as

$$\Psi(r,z,t) \cong \Psi(r_0,z_0,0) + \left(\left. \frac{\partial \Psi_{(i)}}{\partial I_{(j)}} \right|_{I=I_0} \right) \delta I \tag{8.3}$$

where $\left(\left. \frac{\partial \Psi_{(i)}}{\partial I_{(j)}} \right|_{I=I_0} \right)$ is the matrix with elements (I, j), which determines the flux deviation in circuit i at the unit current deviation in circuit j at time $t = 0$.

Taking into account Eq. (8.3), linearised Eq. (8.2) is written as follows:

$$\frac{d}{dt}\left(\left.\frac{\partial\Psi_{(i)}}{\partial I_{(j)}}\right|_{I=I_0}\delta I\right)+R\delta I=\delta U, \tag{8.4}$$

to describe the dynamics of current deviations in circuits $\delta I(t)$.

The ψ flux is a linear combination of the flux through circuit, ψ_{ext}, from external currents and the own current, and the flux from plasma, ψ_p. The ψ_p value is determined by changes in the plasma shape and the plasma's own current (here and throughout, changes in the shape refer to the plasma column movement and deformation). In a linear approximation

$$\Psi_p(r,z,t)\cong\Psi_p(r_0,z_0,0)+\left.\frac{\partial\Psi_p}{\partial I_p}\right|_{I=I_0}(\delta I)+\left.\frac{\partial\Psi_p}{\partial I_p}\right|_{I=I_0}\left(\delta I_p\right), \tag{8.5}$$

where $\left.\frac{\partial\Psi_{p(i)}}{\partial I_{(j)}}\right|_{I=I_0}$ is the matrix with elements (i,j), which determines flux deviations in circuit i due to the plasma shape changes at the unit current deviation in circuit j at time $t = 0$, and $\left.\frac{\partial\Psi_p}{\partial I_p}\right|_{I=I_0}$ is the vector with elements (i), which determines changes in flux deviation in circuit i at the unit plasma current deviation at time $t = 0$.

From Eq. (8.5) we see that a linear model must include state δI_p – the plasma current deviation from the initial value. Then, Eq. (8.4) becomes

$$\left.\frac{\partial\Psi_{ext(i)}}{\partial I_{(j)}}\right|_{I=I_0}\frac{d}{dt}(\delta I)+\left.\frac{\partial\Psi_p}{\partial I}\right|_{I=I_0}\frac{d}{dt}(\delta I)+\left.\frac{\partial\Psi_p}{\partial I_p}\right|_{I=I_0}\frac{d}{dt}\left(\delta I_p\right)+R\delta I=\delta U, \tag{8.6}$$

where $\left.\frac{\partial\Psi_{ext(i)}}{\partial I_{(j)}}\right|_{I=I_0}$ is the matrix with elements (i,j), which determines flux deviation in circuit i at the unit current deviation in circuit j at time $t = 0$ (a static inductance matrix). We introduce designations

$$L_1=\left.\frac{\partial\Psi_{ext(i)}}{\partial I_{(j)}}\right|_{I=I_0};L_2=\left.\frac{\partial\Psi_{p(i)}}{\partial I_{(j)}}\right|_{I=I_0};M_p=\left.\frac{\partial\Psi_p}{\partial I_p}\right|_{I=I_0};L_3=L_1+L_2$$

to bring Eq. (8.6) to form

$$L_3\frac{d}{dt}(\delta I)+M_p\frac{d}{dt}\left(\delta I_p\right)+R\delta I=\delta U. \tag{8.7}$$

The linear system (8.7) is one equation short of the number of states. It should be complemented with an equation describing the change of the plasma current δI_p. To this end, we assume, consistently with the MHD theory, that the poloidal flow is 'frozen' into the plasma during the discussed time periods, so that

$$\overline{\Psi} = \frac{1}{I_p}\int_s j\Psi ds = \text{const}, \tag{8.8}$$

where j is the plasma current distribution, and S is the plasma column cross-section. We linearise Eq. (8.8) with respect to the δI and δI_p states, and obtain

$$\frac{\partial\overline{\Psi}}{\partial I}\delta I + \frac{\partial\overline{\Psi}}{\partial I_p}\delta I_p = 0, \tag{8.9}$$

or

$$\delta I_p = -\frac{\partial\overline{\Psi}}{\partial I}\delta I \Big/ \frac{\partial\overline{\Psi}}{\partial I_p}. \tag{8.10}$$

Through the substitution of Eq. (8.10) into Eq. (8.7) the latter becomes

$$L^*\frac{d}{dt}(\delta I) + R\delta I = \delta U, \tag{8.11}$$

where $L^* = L_3 - M_p[(\partial\overline{\Psi}/\partial I)/(\partial\overline{\Psi}/\partial I_p)]$. This linear system reflects the current behaviour in active and passive circuits, and Eq. (8.9) describes the plasma current dynamics.

To describe a plasma shape evolution, let us introduce vector $g(t)$ characterising the parameters of plasma shape and position. This vector may include such parameters as the plasma elongation and triangularity, X-point position, distance between the plasma boundary and given points on the first wall, and so on. Then

$$g(t) = \frac{\partial g}{\partial I}\delta I + \frac{\partial g}{\partial I_p}\delta I_p,$$

which leads, through Eq. (8.10), to

$$g(t) = \left(\frac{\partial g}{\partial I} - \frac{\partial g}{\partial I_p}\frac{\partial\overline{\Psi}}{\partial I}\Big/\frac{\partial\overline{\Psi}}{\partial I_p}\right)\delta I. \tag{8.12}$$

We denote $C \equiv \dfrac{\partial g}{\partial I} - \dfrac{\partial g}{\partial I_p}\dfrac{\partial\overline{\Psi}}{\partial I}\Big/\dfrac{\partial\overline{\Psi}}{\partial I_p}$ and thus obtain

$$g(t) = C\delta I. \tag{8.13}$$

We therefore obtain the required MLE describing the dynamics of circuit currents and plasma shape evolution:

$$\begin{cases} L^* \dfrac{d}{dt}(\delta I) + R\delta I = \delta U \\ g(t) = C\delta I. \end{cases} \tag{8.14}$$

Eq. (8.14) allows one to analyse the passive stabilisation efficiency of the structures surrounding the plasma. The characteristic routinely used in this context for vertically elongated plasmas is the plasma instability growth rate (increment), γ. It is defined as a singular positive eigenvalue of the matrix $-(L^*)^{-1}R$, related to the unstable vertical mode. This value largely determines the parameters of power supplies for control by the active coils. Generally, the higher this value, the greater the power supply frequency characteristics and required power for control. Another characteristic routinely employed in the passive stabilisation analysis is the stability margin, m_s. Let us take a close look at it.

For unstable plasma configurations, τ_γ, the inverse of the increment, is defined as a singular positive eigenvalue of MLE (8.14), that is

$$-L^* x_u \equiv (S - L_1) x_u = \tau_\gamma R\, x_u, \tag{8.15}$$

where matrix $L^* \equiv L_1 - S$; matrix $S \equiv -[L_2 - M_p(\partial\overline{\Psi} / \partial I) \,/\, (\partial\overline{\Psi} / \partial I_p)]$; matrix $L_1 = \left.\dfrac{\partial \Psi_{ext(i)}}{\partial I_{(j)}}\right|_{I=I_0}$; R is the resistance matrix, and x_u is the distribution of currents induced by the unstable mode, that is, the eigenvector corresponding to the increment. From Eq. (8.15) follows

$$\tau_\gamma = \frac{x_u^T L_1 x_u}{x_u^T R x_u}\left(\frac{x_u^T S x_u}{x_u^T L_1 x_u} - 1\right). \tag{8.16}$$

We now introduce a 'resistive' stability margin

$$\mu = \frac{x_u^T S x_u}{x_u^T L_1 x_u} - 1, \tag{8.17}$$

and the passive structure's senior time constant

$$\tau_S = \frac{x_u^T L_1 x_u}{x_u^T R x_u} - 1. \tag{8.18}$$

Then, $\tau_\gamma = \tau_S \mu$. From Eq. (8.18) follows that the passive structure's senior time constant is an averaged value that can be unambiguously determined by the x_u. We note that μ depends on the conductors' resistance through the x_u.

To pass to the 'inductive' version of the stability margin, we substitute matrix R in Eq. (8.15) with matrix $L_1 = \left.\dfrac{\partial \Psi_{ext(i)}}{\partial I_{(j)}}\right|_{I=I_0}$ and find the eigenvalues m_i and the eigenvectors x_i in the problem:

$$-L^* x_i \equiv (S - L_1) \quad x_i = m_i L_1 x_i, \tag{8.19}$$

where index i runs over values from 1 to the number of states in the system. From Eq. (8.19) it follows that

$$m_1 = \frac{x_i^T S x_i}{x_i^T L_1 x_i} - 1. \tag{8.20}$$

If any matrix (including L^*) is multiplied by a positive definite matrix (L_1^{-1} or R), there are no changes to the number of positive or negative eigenvalues, so there is only one positive m_i value for one positive unstable mode τ_γ. We denote it as stability margin m_s. If $m_s < 0$, then the plasma is either stable on the passive structures' time constant scale or unstable on an Alfvén timescale.

From Eq. (8.20) it can be shown that the m_s is only dependent on the conductors' geometry. The x_s eigenvector, corresponding to stability margin m_s, determines the in-conductor distribution of currents due to the plasma's instantaneous displacement in the 'instability' direction. In physical terms, the m_s, if normalised, reflects the difference between a stabilising force acting on the plasma by currents induced in ideally conducting passive structures at plasma instantaneous vertical displacements, and a destabilising force due to the plasma 'elongating' by the poloidal field. Therefore, the value m_s determines how close a passive structure has to be to stabilise plasma: the larger the m_s the closer the structure to the plasma. In the design of a control system, $m_s \approx 0.5$ is currently acceptable. We notice that even at large m_s, the τ_γ parameter (more important for the plasma stabilisation) may be small due to a passive structure's poor conductivity. The m_s and τ_γ must be sufficiently high to enable an acceptable level of plasma stabilisation. Simply put, a well-conducting passive structure should be as close to the plasma as the design permits.

The linear model (Eq. (8.14)) is used as a basis for synthesising the controllers of closed-loop control systems. Thus, it allows obtaining transfer matrix $K(s)$ that relates sensor signals identifying the plasma position, current and shape to control coil voltages $U(s) = K(s)g(s)$, with s denoting the Laplace variable.

At the design of the plasma position, current and shape control system, it is also important to determine the plasma's possible disturbances, which should be suppressed by the control system. These include disturbances of the plasma's internal inductance l_i and the β_p parameter, caused by rearrangement of temperature and current profiles at 'minor disruptions.' We introduce such perturbations in our linear model.

Let $\delta\xi$ be a disturbance vector. Then, electro-technical Eq. (8.7) becomes

$$L_3 \frac{d}{dt}(\delta I) + M_p \frac{d}{dt}(\delta I_p) + \frac{\partial \Psi}{\partial \xi} \frac{d}{dt}(\delta \xi) + R\delta I = \delta U. \tag{8.21}$$

Eq. (8.9) reflecting plasma current variations becomes

$$\frac{\partial \overline{\Psi}}{\partial I}\delta I + \frac{\partial \overline{\Psi}}{\partial I_p}\delta I_p + \frac{\partial \overline{\Psi}}{\partial \xi}\delta \xi = 0, \tag{8.22}$$

and the equation describing the plasma geometry becomes

$$g(t)=\frac{\partial g}{\partial I}\delta I+\frac{\partial g}{\partial I_p}\delta I_p+\frac{\partial g}{\partial \xi}\delta\xi. \tag{8.23}$$

Substitution δI_p from Eq. (8.22) into Eqs (8.21) and (8.23), we obtain the desired MLE that accounts for possible disturbances of plasma parameters:

$$\begin{cases} L^*\dfrac{d}{dt}(\delta I)+M_\xi\dfrac{d}{dt}(\delta\xi)+R\delta I=\delta U \\ g=C\delta I+F\delta\xi, \end{cases} \tag{8.24}$$

where

$$M_\xi\equiv\frac{\partial\Psi}{\partial\xi}-M_p\frac{\partial\overline{\Psi}}{\partial\xi}\Bigg/\frac{\partial\overline{\Psi}}{\partial I_p},$$

and

$$F\equiv\frac{\partial g}{\partial\xi}-\frac{\partial g}{\partial I_p}\frac{\partial\overline{\Psi}}{\partial\xi}\Bigg/\frac{\partial\overline{\Psi}}{\partial I_p}.$$

In the theory of controller synthesis, the equations for a control object are routinely written in the A, B, C, D form. From Eq. (8.24) it follows that in our case they will take the form

$$\begin{cases} \dfrac{d}{dt}(\delta I)=A\delta I+B\delta U+E\dfrac{d}{dt}(\delta\xi) \\ g=C\delta I+D\delta U+F\delta\xi, \end{cases} \tag{8.25}$$

where $A\equiv-\left(L^*\right)^{-1}R$, $B\equiv(L^*)^{-1}$, D is the zero matrix, and $E\equiv-\left(L^*\right)^{-1}M_\xi$.

Excluding variable $(d/dt)(\delta\xi)$ by substitution $x\equiv\delta I-E\delta\xi$ we, bring Eq. (8.25) to final form

$$\begin{cases} \dot{x}=Ax+B\delta U+AE\delta\xi \\ g=Cx+D\delta U+(CE+F)\delta\xi. \end{cases} \tag{8.26}$$

Now let us describe the procedure for calculating matrix coefficients of a linear model for a given plasma configuration. Fig. 8.1 shows an example of a plasma configuration and positions of points on separatrix that are used as targets to control the plasma shape. The passive structure is represented schematically by a combination of inner and outer axisymmetric rings inside the vacuum vessel and by the vessel's double shell. As for the control coils, in the linear model they are described by 11 circuits. The inner and the outer rings are segmented into three loops each. The inner and the outer shells of the vacuum vessel are segmented into 25 axisymmetric loops each. As a result, the linear model comprises 67 states (circuits).

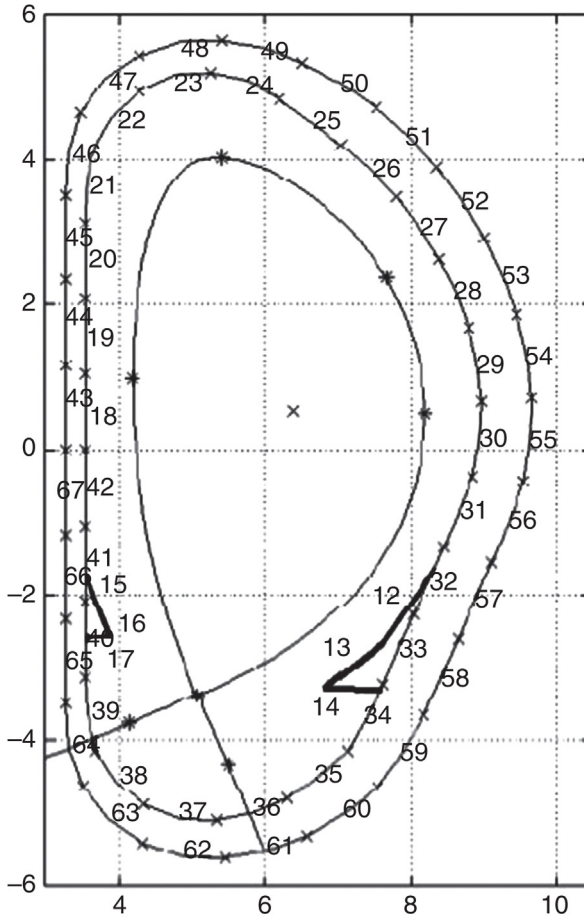

FIGURE 8.1 **Loops in a linear model describing the ITER plasma configuration.** (Copyright ITER Organisation, 2017).

After the states have been identified, we calculate the matrix coefficients using the following algorithm:

a. Calculation of the base plasma configuration using the given poloidal coil currents and plasma parameters. As a rule, basic configurations are derived from snap-shots of discharge scenarios. A base configuration is calculated using free-boundary equilibrium codes.

b. Calculation of the coefficients for matrix $L_3 = \left.\frac{\partial \overline{\Psi}}{\partial I}\right|_{I=I_0}$ (see Eq. 8.7) through relation $L_{3\{i,j\}} \equiv \left\{\left.\frac{\partial \Psi_i}{\partial I_j}\right|_{I=I_0}\right\} \cong \frac{\Delta \Psi_i}{\Delta I_j}$ by varying the j^{th} circuit current relative to the base value. Here, $\Delta\psi_i$ is the flux change in the *ith* circuit

associated with the current variations in the *jth* circuit ΔI_j. A better precision is achieved when several ΔI_j current variations, both positive and negative, are taken and then averaged. Current variations must not lead to any qualitative change in plasma configuration. For instance, when a free-boundary problem is solved, an *X*-point plasma configuration must not become a limiter configuration, and vice versa. As $L_3 = L_1 + L_2$, it is in principle sufficient to determine the $L_2 = \left.\frac{\partial \Psi_p}{\partial I}\right|_{I=I_0}$ matrix coefficients. The $L_1 = \left.\frac{\partial \Psi_{ext}}{\partial I}\right|_{I=I_0}$ matrix is expressed through static inductances that only depend upon the conductors' geometry. Therefore, this matrix can be calculated in advance.

The coefficients of the $M_p = \left.\frac{\partial \Psi_p}{\partial I_p}\right|_{I=I_0}$ matrix in Eq. (8.7) are calculated in a similar way with the difference that the plasma current is varied: $M_{p\{j\}} \equiv \left\{\left.\frac{\partial \Psi_{p,j}}{\partial I_p}\right|_{I=I_0}\right\} \cong \frac{\Delta \Psi_{p,j}}{\Delta I_p}$. Coefficients determined in a similar way are $\left\{\left.\frac{\partial \overline{\Psi}}{\partial I_j}\right|_{I=I_0}\right\} \cong \frac{\Delta \overline{\Psi}}{\Delta I_j}$, $\left\{\left.\frac{\partial \overline{\Psi}}{\partial I_p}\right|_{I=I_0}\right\} \cong \frac{\Delta \overline{\Psi}}{\Delta I_p}$ (see Eq. 8.9) and $\left\{\left.\frac{\partial g_i}{\partial I_j}\right|_{I=I_0}\right\} \cong \frac{\Delta g_i}{\Delta I_j}$, $\left\{\left.\frac{\partial g_i}{\partial I_p}\right|_{I=I_0}\right\} \cong \frac{\Delta g_i}{\Delta I_p}$ (see Eq. 8.12).

The coefficients of the matrices for disturbances factored in the linear model are $\left\{\left.\frac{\partial \Psi_i}{\partial \xi_j}\right|_{I=I_0}\right\} \cong \frac{\Delta \Psi_i}{\Delta \xi_j}$, $\left\{\left.\frac{\partial \Psi_i}{\partial \xi_j}\right|_{I=I_0}\right\} \cong \frac{\Delta g_i}{\Delta \xi_j}$, where the ξ_j disturbance parameter is varied. The ΔIp and $\Delta \xi$ variations too must not lead to any qualitative change in plasma configuration.

c. After the completion of step b), derive the desired linear model in the form of Eq. (8.25) or Eq. (8.26). Simultaneously, analyse the linear model characteristics using the passive stabilisation or active stabilisation criteria (by determining the increment, the stability margin, etc.).

8.4.2 Non-linear Modelling

Non-linear modelling allows one to assess how well certain parameters can be controlled with poloidal field coils using a given power supply system. In addition, nonlinear modelling may be employed to optimise discharge scenarios when planning a plasma experiment. A relevant code should be based on modern transport concepts in the plasma and be validated through experiments on the operative machines.

One of the most advanced codes for accomplishing these aims is the DINA code, developed in Russia [3]. DINA allows accounting in a self-consistent manner for

- 2D free boundary plasma equilibrium
- 1D transport processes for plasma parameters averaged over magnetic flux surfaces.

The vacuum vessel is described by a set of axisymmetric filaments. Currents in the vessel and poloidal field coils are computed self consistently with the evolution of plasma. 2D equilibrium equations are solved with a combination of the conventional finite element method and the variable inversion technique. The transport processes are described by equations for plasma components (H, D, T), electron and ion temperatures and poloidal magnetic flux diffusion. Current drive and bootstrap current models, neutral beam injections (set of filament-like beams), as well as injection of pellets that evaporate fast compared to $\tau_E$have all been included in the DINA code as subroutines.

The code also factors in the effect of eddy currents in the vessel shells on the plasma column evolution. DINA allows modelling the plasma current position and shape control system.

Let us consider the stage-by-stage simulation of a control system at the nonlinear modelling of discharge scenarios [4]. The stage-by-stage approach is also feasible when planning an experiment.

At the first stage, we select preprogrammed (target) parameters to be controlled by feedback loops. For limiter-phase plasma configurations during the current ramp-up and plasma termination phases, these may include the following:

- Velocity of vertical displacements for the stabilisation of the plasma's vertical instability by the fast control loop. For example, vertical displacement time in ITER is 70–200 ms.
- Plasma vertical position (a 'slow' plasma shape control loop). For ITER, the time is a few seconds.
- Gap between the first wall and the point on the plasma boundary with innermost or outermost radius (the 'slow' plasma shape control loop).
- Currents in poloidal field coils (the 'slow' loop).
- Plasma current (the 'slow' loop).

For divertor-phase plasma configurations during the current ramp-up, flat top and plasma termination phases, these may include the following:

- Velocity of vertical displacements for the stabilisation of the plasma's vertical instability by the fast control loop.
- Gaps between the first wall and the points on the plasma boundary mainly affecting the plasma performance (the 'slow' plasma shape control loop).

- Currents in poloidal field coils (the 'slow' loop).
- Plasma current (the 'slow' loop).

Plasma shape control parameters and their number differ for limiter-phase and divertor-phase plasma configurations. It is therefore reasonable to employ different controllers for the phases with a smooth transition from one configuration control to another.

Programmed values of these parameters are derived from static calculations, as they enable optimisation of mechanical loads on the poloidal magnetic system and the tokamak power supply. As a matter of fact, a static scenario determines the evolution of the plasma shape and poloidal coil currents, which the control system will have to provide. In addition, a static scenario allows specifying the programmed values of poloidal coil voltages needed to obtain given coil currents and a plasma current during a discharge.

At the second stage, we embed a specific CLCS into the simulation code. This includes a programmed description of control laws (controllers) for limiter and divertor plasma configurations, a simplified description of coil power supply and different control algorithms.

Then, we perform the first iteration of discharge simulations and correct the programmed values of poloidal coil voltages. Where necessary, we adjust controller coefficients at the same simulation stage. As a rule, simulation results indicate control parameters that need to be adjusted to improve the control performance. The improvement is achieved through a linear-model-based new controller synthesis by selecting weights such that particular parameters could become better 'controllable' or by changing the computation algorithm for such parameters, if possible. Then, we perform the second iteration of discharge simulations and adjust the control system additionally, if necessary.

8.5 ANALYTICAL SYNTHESIS AND CONTROL SYSTEM OPTIMISATION

8.5.1 Basic Concept

An analytical rationale of the logic of plasma stabilisation in the vicinity of equilibrium position is based on modern approaches to mathematical modelling and design of closed-loop control systems [5].

One of the basic features of such approaches is that they are concerned with mathematical optimisation problems involving different metric spaces. Number one is the problem of asymptotic stability by Lyapunov. In the vast majority of cases, Lyapunov stability is achieved in more than one way. So, the second requirement is that a certain numerical characteristic of the 'dynamic process quality' is optimised.

A formalised approach requires that the desired elements of a designed system be formed based on the solutions to the mentioned optimisation

problems. Such approaches are premised on formalised ideas about a control system's performance. This formalisation implies that there exists a set of quantitative characteristics describing performance, whose values are determined by design solutions. Such characteristics may include various functionals specified in relevant metric spaces. If, for example, the spaces of sought-for elements are normalised, relevant norms may be used as quality functionals.

In dealing with a closed-loop stabilising system, the 'dynamic process quality' is reduced to the use of matrix norms for a quantitative evaluation of the transfer matrices. This evaluation allows us to understand how large output signals are relative to certain classes on input signals. If the input signals are disturbances making plasma's dynamic parameters deviate from equilibrium, the stabilisation quality depends on how well the control system suppresses them. The suppression effectiveness, in turn, depends on the values of transfer matrix norms: the smaller the norm the higher the suppression effectiveness. In this context, the optimal stabilisation problem may be interpreted as the choice of a feedback controller capable of minimising a relevant transfer matrix norm.

8.5.2 Problem Generalisation

Let us assume that a plasma column numerical simulation is described by a system of ordinary nonlinear differential equations

$$\dot{x} = F(x, u, \varphi), \tag{8.27}$$

defined on positive time semiaxis $t \in (0, \infty)$. Here, $x \in E^n$ is the vector of the object's state, $u \in E^m$ is the vector of control actions, and $\phi \in E^l$ is the vector of disturbances acting on the object under control. We assume that the F vector function in the right-hand side satisfies the conditions of the existence and uniqueness of the solution of the Cauchy problem for Eq. (8.27).

We further introduce vector functions $x = x_p(t)$, $u = u_p(t)$ and $\phi = \phi_p(t)$ that determine the controlled dynamics of the object and satisfy Eq. (8.27)

$$\dot{x}_p = F\left(t, x_p, u_p, \varphi_p\right).$$

For the purposes of our control system, dynamics of the plasma's equilibrium position is assumed to be a controlled movement. We denote deviations of respective variables from a controlled movement as $x = x(t)$, $u = u(t)$, and $\phi = \phi(t)$, where $x(t) = x_p(t) + x(t)$, $u(t) = u_p(t) + u(t)$, and $\phi(t) = \phi_p(t) + \phi(t)$. Substitution of these relations into the original Eq. (8.27) gives the equation for a disturbed plasma movement, expressed as deviations from equilibrium position:

$$\dot{x} = G\left(t, x, u, \varphi\right), \tag{8.28}$$

where $G(t, x, u, \varphi) = F(t, x_p + x, u_p + u, \varphi_p + \varphi) - F(t, x_p, u_p, \varphi_p)$.

We further introduce a linear mathematical model of the controller:

$$u = W(s)\,Cx, \tag{8.29}$$

where C is a constant matrix under a given measurement law, and $W(s)$ is the transfer matrix of the controller. We also introduce a linearised system (8.28), expressed as deviations from the equilibrium position:

$$\dot{x} = Ax + Bu + H\varphi, \tag{8.30}$$

where matrices A, B and H have constant components. The (8.29) controller is considered to be stabilising the zero equilibrium position of system (8.28) or the system's controlled movement (8.27) under the assumption that the zero equilibrium position of systems (8.28) and (8.29) is asymptotically stable in the sense of Lyapunov.

We know that controlled movement $x = x_p(t)$, $u = u_p(t)$ and $\phi = \phi_p(t)$ (or the zero equilibrium position of system (8.28)) can be made asymptotically stable in the sense of Lyapunov using the feedback control given by Eq. (8.29). To accomplish this, it is necessary that condition $\| G(t,x,u,0) - A(t)x - B(t)u \| \leq \theta(\| x \| + \| u \|)$, (at $\phi(t) \equiv 0$, and where $\theta \to 0, \| x \| \to 0, \| u \| \to 0$) is satisfied, and that the uncontrolled part of the (8.30) linear approximation is stable.

The second requirement is certainly met if controllability, in the sense of Kalman, exists, that is, rank $(B\ AB\ A^2B \ldots A^{n-1}\ B) = n$. If the (8.29) controller ensures that the roots of characteristic polynomials of the (8.29), (8.30) closed-loop system lie in the open left semiplane, this controller is considered to be stabilising the zero equilibrium state of system (8.28) or the system's controlled movement (8.27).

Infinitely many controllers stabilising a given controlled movement may be involved in satisfying the stated conditions. It is therefore logical to introduce the quantitative characteristics of stabilisation quality. To this end, on the movements of a closed-loop system, expressed through Eqs (8.27) and (8.29) as

$$\begin{cases} \dot{x} = F[t, x(t), u(t), \varphi_p(t) + \varphi(t)] \\ u = u_p(t) + W)(p)[x(t) = x_p], \end{cases} \tag{8.31}$$

where $p = d/dt$ is a differential operator, we specify some non-negative functional

$$I_H = [x(t), u(t)].$$

With the (8.31) closed-loop system's initial conditions being similar, and the $\phi(t)$ functional being equal, the I_H functional depends upon the choice of transfer matrix $W(s)$ of the (8.29) controller. Hence,

$$I_H = \{x[t, W(p)], u[t, W(p)]\} = I_H\,[W(p)] = I_H(W).$$

The $u = W^0(p)x$ controller is said to be optimal relative to the I_H functional, if the controller (8.29) stabilises the considered system in the sense of Lyapunov and minimises the value of functional $I_H(W)$.

The problem in the analytical synthesis of a linear controller is actually a search for a stabilizing controller, optimal relative to the I_H functional:

$$I_H = I_H(W) \to \min_{W \in \Omega}.$$

Here, Ω is an ensemble of transfer matrices for controllers of the (8.29) form, that is, matrices of dimensions' m by k with rational fraction components such that the characteristic polynomial of Eqs (8.29) and (8.30) closed-loop system is unambiguously Hurwitzian.

As one can see, the main purpose of the analytical synthesis is to find a linear controller able to optimise a nonlinear system's movement. However, we emphasise that optimisation techniques using fully linear models are particularly important in the design of plasma stabilisation systems. Let us consider this in greater detail.

We express a model of a linear time-invariant control system (LTI model) as a state-space representation of the form

$$\begin{aligned} \dot{x} &= Ax + Bu + Gd; \\ e &= Lx + Mu + Nd; \\ y &= Cx + Du + Fd, \end{aligned} \tag{8.32}$$

where $x \in E^n$ is the vector of state, $e \in E^p$ is the vector of controlled outputs, $y \in E^k$ is the measurement vector, $u \in E^m$ is the vector of control actuators and $d \in E^l$ is the vector of disturbances. A, B, C, D, F, G, L, M and N are the constant matrices of respective dimensions. Taking constant vectors (d/u) and (e/y) as the input and output signals respectively, we can transform the LTI model (for the frequency domain) into the equivalent form

$$\begin{pmatrix} e \\ y \end{pmatrix} = P(s) \begin{pmatrix} d \\ u \end{pmatrix}, \tag{8.33}$$

where $P(s)$ is the transfer matrix of the control object (Fig. 8.2). We further introduce an LTI model, which can be written either in the form of a state-space representation

$$\begin{aligned} \dot{\xi} &= A_c\xi + B_c y; \\ u &= C_c\xi + D_c y, \end{aligned} \tag{8.34}$$

with $\xi \in E^{n_c}$ denoting the vector of the controller's states, or in the form of the input–output

$$u = K(s)y. \tag{8.35}$$

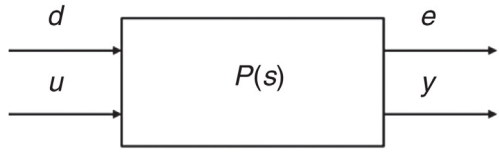

FIGURE 8.2 Block diagram of the LTI model.

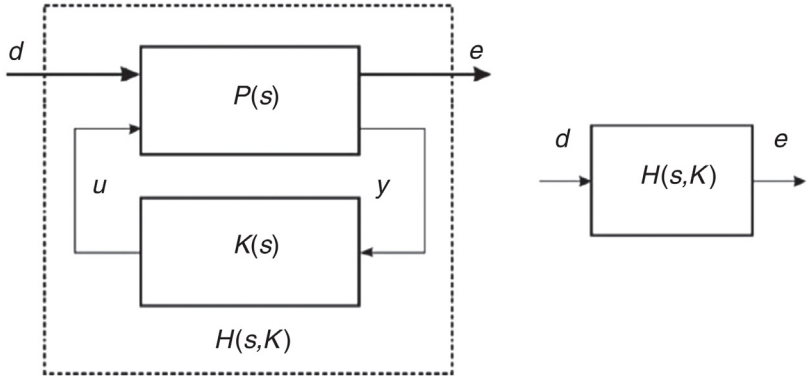

FIGURE 8.3 Block diagram of a closed-loop system.

Eqs (8.32) and (8.35) are written in the form of Laplace transformation (at zero initial conditions). We close the control object using the mentioned controller (Fig. 8.3).

We remember that the purpose of an optimised synthesis of a control system is to find an either Eq. (8.34) or Eq. (8.35) controller allowing the system to be stable and minimising the functional that characterises its dynamic properties. Through Eqs (8.32) and (8.35) one can easily obtain the following expressions for the transfer matrices of control object $P(s)$, controller $K(s)$ and closed-loop system системы: $H(s, K)$

$$P(s)=\left(\begin{array}{c|c} L(Es-A)^{-1}B+M & L(Es-A)^{-1}G+N \\ \hline C(Es-A)^{-1}B+D & C(Es-A)^{-1}G+F \end{array}\right);$$

$$K(s)=C_C\left(E_{n_C}s-A_C\right)-1B_C+D_C$$

$$\begin{aligned} H(s,K)&=L(Es-A)^{-1}B+M \\ &+\left[L(Es-A)^{-1}G+N\right]\left[E_m-K(CEs-A)^{-1}G-KF\right] \\ &K\left[C(Es-A)^{-1}B+D\right]. \end{aligned}$$

In these formulas, E, E_{n_c} and E_{m} denote identity matrices of dimensions $n \times n$, $n_c \times n_c$, and $m \times m$. The $H(s, K)$ matrix may be interpreted as a gener-

alised gain matrix of the 'external input disturbances d – generalised output vector e' loop. As external disturbances lead to deviation of the plasma's dynamic parameters from their equilibrium values, the stabilisation effectiveness depends on how well the control system suppresses them. The lower the $H(s, K)$ gain matrix the higher the stabilisation effectiveness.

In this connection, it makes sense to solve a problem of the maximum degree of suppression of external disturbances through minimisation of the $H(s,K)$ gain matrix by optimal choice of transfer matrix of the $K(s)$ controller. To accomplish this, it is necessary to formalise the requirement that the $H(s, K)$ transfer matrix should be 'small.' To this end, we can use a matrix norm $\left\|H(s,K)\right\|$ as a functional to be minimised. Then, a generalised problem of the maximum degree of suppression of external disturbances may be expressed as

$$I = I(K) = \left\|H(s,K)\right\| \to \inf_{K \in \Omega}, \tag{8.36}$$

where Ω is an ensemble of transfer matrices with rational fraction components, for which the characteristic polynomial of the (8.33), (8.35) closed-loop system is unambiguously Hurwitzian.

The choice of specific norm in Eq. (8.36) is associated with different classes of problems dealing with the optimised synthesis of a stabilising controller. Currently, problems that have to be dealt with most often include the following [6]:

- $\|H\|_2$ norm minimisation problem (typically represented by the LQG-optimal synthesis problem),
- $\|H\|_\infty$ norm minimisation problem (the H_∞-optimal synthesis problem), and
- the problem of minimisation of the first two norms for 'weighted' transfer matrices HS_1, where $S_1(s)$ is a given weighted matrix function; examples include root mean square optimal synthesis problems and ensuring controller synthesis problems.

Going forward, we assume that all the roots of the characteristic polynomial of the closed-loop system, mathematically expressed by Eqs (8.33) and (8.35), lie in the open left semiplane. We also assume that for all transfer matrices, $H(s)$, discussed later, expression $tr\left[H^T(-s)H(s)\right]$ is a proper rational fraction. Then, the given norms are introduced through

- norm $\left\|H\right\|_2$:

$$\left\|H\right\|_2 = \sqrt{\frac{1}{2\pi}\int_{-\infty}^{\infty} tr\left[H^T(-j\omega)H(j\omega)\right]d\omega}. \tag{8.37}$$

For example, for the single-input single-output (SISO) *d/e* problem

$$\left\|H\right\|_2 = \sqrt{\frac{1}{2}\int_{-\infty}^{\infty}\left|H(j\omega)\right|^2 d\omega}; \tag{8.38}$$

- norm $\|H\|_\infty$:

$$\|H\|_\infty = \max_{\omega\in[0,\infty)} \bar{\sigma}(\omega), \tag{8.39}$$

where $\bar{\sigma}(\omega)$ is the maximum singular value of matrix $H(j\Omega)$, that is, the square root of the maximum eigenvalue of hermitian matrix $H^T(-J\Omega)H(J\Omega)$. For the SISO problem

$$\|H\|_\infty = \max_{\omega\in[0,\infty)} |H(\omega)|; \tag{8.40}$$

- weighted norm $\|HS_1\|_2$

$$\begin{aligned}\|HS_1\|_2 &= \sqrt{\frac{1}{2\pi}\int_{-\infty}^{\infty} tr\left[S_1^T(-j\omega)H^{\mathrm{T}}(-j\omega)H(j\omega)S_1(j\omega)\right]d\omega} \\ &= \sqrt{\frac{1}{2\pi}\int_{-\infty}^{\infty} tr\left[H(j\omega)S_1(j\omega)S_1^T(-j\omega)H^T(-j\omega)\right]d\omega}, \\ \|HS_1\|_2 &= \sqrt{\frac{1}{2\pi}\int_{-\infty}^{\infty} \mathrm{tr}\left[H(j\omega)S_v(\omega)H^T(-j\omega)\right]d\omega},\end{aligned} \tag{8.41}$$

where $S_v(\omega) = S_1(j\omega)S_1^T(-j\omega)$. For the SISO problem

$$\|HS_1\|_2 = \sqrt{\frac{1}{2\pi}\int_{-\infty}^{\infty} |H(j\omega)|^2 S_v(\omega)d\omega}, \tag{8.42}$$

where weighted norm $\|HS_1\|_\infty$

$$\|HS_1\|_\infty = \max_{\omega\in[0,\infty)} \bar{\sigma}_v(\omega) \tag{8.43}$$

where $\bar{\sigma}_v(\omega)$ is the maximum singular value of matrix $H(j\omega)S_1(\omega)$.

8.6 PLASMA START-UP PHASE

8.6.1 Dynamics of Tokamak Electromagnetic Processes

Simply put, the tokamak plasma start-up includes the breakdown of the fuel gas mixture, subsequent ramp-up of the generated plasma current and formation of closed magnetic flux surfaces. The start-up phase is paid particular attention to at the design of the tokamak power supply and control systems.

First, the vortex electric field and acceptable stray magnetic fields required for plasma breakdown specify the critical operational conditions for the power supply of poloidal field coils (PFCs). Second, at the start-up phase the ionisation and radiation 'barriers' should be overcome. For this purpose the auxiliary heating (electron cyclotron resonance power) can be used. These challenges make the transient plasma control problem a special case of mathematical modelling.

The transient processes in tokamaks are described by a system of ordinary differential equations, which can be written in a matrix form as

$$\frac{d(LI)}{dt} + RI = U, \tag{8.44}$$

where L is the inductance matrix, I is the vector of circuit currents, R is the diagonal matrix of the circuits' resistances, and U is the vector of power supply voltages. The L inductance matrix is determined entirely by the conductive elements' geometry. In the context of an axisymmetric description, the conductive elements are modelled as a system of axisymmetric loops. This applies to the PFCs and the vacuum vessel and other conductive passive structural components. The conductive shell structural components are all modelled using the finite-element method. The elements of the R diagonal matrix are determined by the electrical resistance of the respective structural materials. The model should also include the mathematical description of the PFCs' power supply.

The goal of the problem is to find such PFCs' voltage- time dependencies, which would ensure realisation of optimal breakdown conditions at the breakdown time, that is the simultaneous formation of the electrical field with the required voltage and compensated stray magnetic fields. The latter, generally, should be within 2 mT in the breakdown region. The need to provide the plasma equilibrium imposes additional constraints on the poloidal magnetic field. Starting from breakdown, the magnetic field horizontal component must be kept close to zero to avoid major plasma vertical displacements. At the same time, its vertical component must remain consistent with the magnetic equilibrium field corresponding to the given plasma major radius and current (Shafranov field). These requirements may be written as follows:

$$\begin{aligned} &\left\langle B_z(R,Z)\right\rangle \approx 0 \\ &\left\langle B_z(R,Z)\right\rangle + \frac{\mu_0 I_p}{4\pi r}\left[\ln\left(\frac{8R}{a} + \beta_p + \frac{l_i}{2} - \frac{3}{2}\right)\right] \approx 0. \end{aligned} \tag{8.45}$$

To sum it up, the magnetic field in the breakdown region must provide the plasma in stable equilibrium in the vertical and horizontal directions. This is especially important during the plasma initiation stage, when the plasma current is relatively small. The plasma column's circular cross-section, preferable at this stage, can be achieved, if the decay index of the magnetic field in the breakdown region $< n >= -(R/ < B_z >) \times (d < B_z > /dR)$ is close to 0.5.

In addition, the model should account for the constraints on the values of PFCs' currents and voltages, which depend on the choice of a power supply system and adopted design solutions. Other constraints are possible depending on specific operational requirements, design features and characteristics of auxiliary equipment.

The described logical model underlies the TRANSMAK computational code, used to design and simulate the scenarios of the start-up phase. Mathematically, the problem is reduced to a system of linear finite-difference equations with constraints. It is solved using a simplex method in which the magnetic flux in the breakdown region at the breakdown time is maximised.

8.6.2 Plasma Transport Model at Start-Up Phase

The TRANSMAK code uses a zero-dimensional multicomponent transport model (named SCENPLINT – SCENario of PLasma INitiation in Tokamaks – code) to assess the plasma column ohmic resistance. The SCENPLINT code represents further development of the code described in Ref. [7]. In comparison with Ref. [7] the SCENPLINT code takes into account the following:

- Several types of impurities (Be, C, O, Fe, W) with 0D equations for their ionisation states evolution, radiation and sources (S_Z) of impurities given by the physical sputtering model or by the phenomenological one. For beryllium impurity, for instance, evolution of ionisation states is described by

$$\left.\begin{aligned}\frac{dn_{Be,0}}{dt} &= n_e\left(n_{Be,1}R_{Be,1} - n_{Be,0}I_{Be,0}\right) + n_0 n_{Be,1}X_{Be,1} - \frac{n_{Be,0}}{\tau_{zloss}} + S_{Be}\\ \frac{dn_{Be,j}}{dt} &= n_e\left[n_{Be,j-1}I_{Be,j-1} + n_{Be,j+1}R_{Be,j+1} - n_{Be,j}\left(I_{Be,j} + R_{Be,j}\right)\right]\\ &\quad + n_0\left(n_{Be,j+1}X_{Be,j+1} - n_{Be,j}X_{Be,j}\right) - \frac{n_{Be,j}}{\tau_{zloss}}\\ \frac{dn_{Be,4}}{dt} &= n_e\left(n_{Be,3}I_{Be,3} - n_{Be,4}R_{Be,4}\right) - n_0 n_{Be,4}X_{Be,4} - \frac{n_{Be,j}}{\tau_{zloss}}\end{aligned}\right\}, \qquad (8.46)$$

  where $I_{Be,j}$, $R_{Be,j}$ and $X_{Be,j}$ are ionisation, recombination and charge-exchange rate coefficients; S_{Be} is impurity source; and τ_{zloss} is impurity confinement time (usually $\tau_{zloss} = \tau_E$).
- The model for runaway current I_{R} evolution by Dreicer generation and avalanche multiplication. In this case the equation for plasma current takes the form

$$L_p\frac{dI_P}{dt} = U_{ext} - U_{res} \qquad (8.47)$$

where U_{ext} is external voltage evolution (usually is taken from TRANSMAK code), $U_{res} = R_{pl}\cdot(I_P - I_R)$ is resistive voltage on plasma loop and L_p is plasma inductance.

- Plasma energy confinement model (τ_E), which describes the transition from losses along the magnetic field (τ_{str}) to Bohm losses (τ_{Bohm}) and to L-mode scaling (τ_E^L):

$$\begin{aligned}
&\text{-if } q > 11 \qquad \frac{1}{\tau_E} = \frac{\exp\left(-\dfrac{I_p}{I_{crit}}\right)}{\tau_{str}} + \frac{1}{\tau_{Bohm}} \\
&\text{-if } 9 < q < 11 \qquad \frac{1}{\tau_E} = \frac{1-f(q)}{\tau_{Bohm}} + \frac{f(q)}{\tau_E^L};\ f(q) = 5.5 - 0.5 \times q; \\
&\text{-if } q < 9 \qquad \tau_E = \tau_E^L.
\end{aligned} \tag{8.48}$$

Here, q is safety factor, I_{crit} is the so-called critical current for closed magnetic surfaces formation ($I_{crit} \approx 100$ kA for ITER case).

The SCENPLINT code is described in more detail in an educational book [8], where numerous examples of code application to the analysis of plasma initiation stage in tokamaks (for real experiments on Globus-M, T-10, JT-60U, Tore Supra, KSTAR tokamaks and also for the ITER project) are given.

The transport model used in the SCENPLINT code is a system of ordinary differential equations for electron and ion temperatures (T_e and T_i, respectively), neutral gas concentration (n_e), plasma current (I_p) and 'runaway' electron current (I_R). The pre-breakdown fuel mixture pressure p and ionisation γ_0 are used as initial conditions. These data are used to determine the initial concentration of the fuel mix n_{00} (10^{20} m^{-3}) = 4.8 p (P, and concentration of plasma electrons $n_{e0} = \gamma_0 n_{00}$ ($\gamma_0 \sim 10^{-3}$ to 10^{-2}). Electron and ion initial (T_{e0} and T_{i0}, respectively) are usually (1–2) eV. Other parameters to be set up are the breakdown region geometry (R, a, k), the toroidal magnetic field (B_{t0}), the vortex electric field E in that region, the vacuum vessel volume (V_v); stray magnetic fields at the breakdown time (B_s); the additional ECR heating (Q_{ECRH}), and the parameters characterising the plasma confinement and the dynamics of the plasma impurities.

The mentioned model underlies the SCENPLINT code that has been developed as part of the TRANSMAK code package for the simulation of plasma initiation processes. For SCENPLINT simulations, it is necessary to specify the discharge key characteristics, such as the time dependencies of loop voltage U_{ext} (t) or plasma current $I_p(t)$, the breakdown region geometry and the plasma intrinsic inductance. The SCENPLINT can also be used to pre-select the plasma initial pressure and required auxiliary heating power. These parameters are employed by the TRANSMAK code as input data.

8.7 CORRECTION OF ERROR FIELDS

8.7.1 Effect of Error Fields on Plasma Processes

In tokamaks the poloidal magnetic field minor deviations from the ideal axial symmetry with amplitudes $B_{m,n} / B_{t0} \leq 10^{-4}$ (error fields) may give rise to the so-called locked (i.e. non-rotating) modes. Values $B_{m,n}$ are amplitudes of Fourier harmonics of the normal component of a magnetic field on the plasma rational magnetic surfaces $q = m/n$ (the safety factor) with m poloidal and n toroidal numbers.

Low-order error field modes, such as (1.1), (2.1) and (3.1), interact with the rational q surfaces in the plasma and drive the formation of magnetic islands. If islands are not stabilised, they slow down the plasma rotation and, if the natural rotation is insufficient, the rotating MHD mode locks and the adverse effect of error fields is amplified. The locked modes may considerably limit the operating domain of any tokamak, resulting in a degraded energy/particle confinement or a plasma current disruption not only at the early discharge stage, but also at later discharge stages. A systematic study of the locked mode evolution mechanism allowed a semi-empirical estimation of the acceptable level of error fields (and how to correct them).

As the plasma 'sensitivity' to the locked modes tends to grow with increasing the major radius and toroidal field of tokamaks, this problem is likely to be much more serious for reactor-scale machines, including ITER, than for experimental devices. In the case of ITER, it can be solved if the following requirements are met simultaneously:

- High precision of the magnet manufacturing and assembly,
- Comprehensive accounting and, where possible, elimination of factors that may disturb the field axial symmetry, and
- Presence of correction coils.

Extrapolation of experimental data for a combination of error field modes (m, n) = (1,1), (2,1), (3,1) for the $B_{m,n}$ normal component of error fields to ITER parameters allowed the following multi-mode criterion (referred to as the locked mode threshold or LMT) to be formulated for Ohmic operation at low plasma density:

$$\begin{aligned} B_{\text{3-mode}} &= \sqrt{W_{11} \cdot B_{1,1}^2 + W_{21} \cdot B_{2,1}^2 + W_{31} \cdot B_{3,1}^2}, \\ &\leq 5 \times 10^{-5} \cdot B_{t0} \end{aligned} \tag{8.49}$$

where assigned weights $W_{11} = 0.2$, $W_{21} = 1.0$, $W_{31} = 0.8$, respectively; $B_{t0} = 5.3$ T is the toroidal field at the major radius $R = 6.2$ m. As one can see, the LMT criterion imposes considerable restrictions on error fields in tokamak reactors. Experimentally, it is found that the locking mode (m,n) = (2,1) is the most dangerous and, accordingly, attention is focused on minimising and correcting this error field component. The "3-mode" error field criterion and criteria on the

"overlap" error fields give for ITER case ($R_0 = 6.2$ m) minimum value $B_{error}/B_{t0} \leq 5 \times 10^{-5}$ [9].

8.7.2 Field Perturbation Harmonic Analysis

Error fields are determined in two stages on the basis of the Fourier analysis using magnetic flux co-ordinates. At the first stage, the normal field B is calculated on the $q = 2$ magnetic surface described as

$$\Psi(x, y, z) = \text{const}, \; q = (m / n) = 2 / 1. \tag{8.50}$$

The magnetic flux $\Psi(x, y, z)$ is produced by the poloidal magnet system and the plasma current and can be evaluated in a plasma discharge scenario using the Grad–Shafranov equation. The safety factor is expressed as

$$q = \frac{1}{2\pi} \oint dl \, \frac{B_t(l)}{R(l) \cdot B_p(l)}, \tag{8.51}$$

where dl is the poloidal increment of a field line length; $B_p(l)$ and $B_t(l)$ are the respective poloidal and toroidal fields on the surface $\Psi[X(l), Y(l), Z(l)] = \text{const}$; $R(l)$ is the distance between the point $[X(l), Y(l), Z(l)]$ and the tokamak axis.

The toroidal field is evaluated as

$$B_t(l) = \frac{\mu_0 I_t}{2\pi R(l)}. \tag{8.52}$$

On unperturbed magnetic field lines $[X(l), Y(l), Z(l)]$, the toroidal angle ϕ and the poloidal angle θ are related linearly by

$$\phi(l) = \phi(0) - q \cdot \theta(l) = \text{const}; \tag{8.53}$$

$$X(l) = R(l) \cdot \cos\phi(l); \tag{8.54}$$

$$Y(l) = R(l) \cdot \sin\phi(l). \tag{8.55}$$

The poloidal angle θ is defined by the equation

$$\theta(l) = 2\pi \times \int_{l_0}^{l} \frac{dl}{R^2(l) \cdot B_p(l)} \Big/ \oint \frac{dl}{R^2(l) \cdot B_p(l)} \tag{8.56}$$

or through the safety factor q:

$$\theta(l) = \frac{1}{q} \int_{l_0}^{l} \frac{dl \cdot B_t(l)}{R(l) \cdot B_p(l)} \tag{8.57}$$

The field $B_\perp$ normal to the surface $\Psi\,[X(l), Y(l), Z(l)] = \text{const}$ is determined as

$$B_\perp = (B \nabla \psi) \,/\, |\, \nabla \psi \,|. \tag{8.58}$$

At the second stage, the component $B_{\perp}$ $[R(l),Z(l),\phi(l)]$ on the $q = 2$ surfaces is decomposed into a double Fourier series. The amplitudes $B_{m,n}$ on unperturbed magnetic field lines are

$$B_{m,n} = B_{m,n}^{(c)} + i \times B_{m,n}^{(s)}, \tag{8.59}$$

$$B_{m,n} = \frac{1}{2\pi^2} \oint d\phi \oint d\theta(l) \cdot B_{\perp}[R(l), Z(l), \phi(l)] \cdot \exp\{i[n\phi(l) - m\theta(l)]\}, \tag{8.60}$$

$$(m,n) = (1,1),(2,1),(3,1).$$

Amplitude $B_{m,n}^{(0)}$ and phase $\Psi_{m,n}$ of the resonance harmonic on the $q = 2$ rational surface are expressed through the cosine and sine amplitudes $B_{m,n}^{(c)}$, $B_{m,n}^{(c)}$:

$$B_{m,n}^{(0)} = \sqrt{\left(B_{m,n}^{(c)}\right)^2 + \left(B_{m,n}^{(s)}\right)^2} \tag{8.61}$$

$$\Psi_{m,n} = arctg(B_{m,n}^{(s)}) \,/\, B_{m,n}^{(c)}. \tag{8.62}$$

A Fourier analysis of error fields [10] produced by the poloidal and toroidal magnet systems may be performed using the matrix method. For instance, the following relations hold for toroidal coil error fields:

$$\begin{pmatrix} b_{m,n}^{(c,k+1)} \\ b_{m,n}^{(s,k+1)} \end{pmatrix} = \begin{pmatrix} \cos\phi_t & -\sin\phi_t \\ \sin\phi_t & \cos\phi_t \end{pmatrix} \begin{pmatrix} b_{m,n}^{(c,k)} \\ b_{m,n}^{(s,k)} \end{pmatrix}, \tag{8.63}$$

where $\phi_t = 20$ degrees is the angle between adjacent toroidal coils, and k is the coil number.

The main contributor to error fields is assembly and manufacture errors of the toroidal and poloidal field coils**.** The resultant contribution of the coils to the (m,n) error fields is determined by summing up the respective sine and cosine amplitudes $B_{m,n}^{(c)}$,$B_{m,n}^{(s)}$ of error fields. For the ITER poloidal magnet system, this procedure, accounting for the individual deviations of the coils, is described as

$$\begin{aligned} B_{m,n}^{(c,s)}(pol) = & \sum_{i=1}^{12} b_{m,n}^{(c,s)} \cdot \left[\phi_i'; \delta'(\phi_i')\right] \cdot \delta(\phi_i')\big|_{\phi_i'=0} \times I_i \\ & + \sum_{i=1}^{12} b_{m,n}^{(c,s)} \cdot \left[\phi_i'; \delta'(\phi_i')\right] \cdot \delta(\phi_i')\big|_{\phi_i'=\pi/2} \times I_i \\ & + \sum_{i=1}^{12} b_{m,n}^{(c,s)} \cdot \left[\phi_i'; \omega'(\phi_i')\right] \cdot \omega(\phi_i')\big|_{\phi_i'=0} \times I_i \\ & + \sum_{i=1}^{12} b_{m,n}^{(c,s)} \cdot \left[\phi_i'; \omega'(\phi_i')\right] \cdot \omega(\phi_i')\big|_{\phi_i'=\pi/2} \times I_i, \end{aligned} \tag{8.64}$$

where I_i are the ampere-turns of the poloidal coils and the central solenoid sections, and $b_{m,n}^{(c,s)}$ are the (m,n) error fields caused by unit deviations δ', ω' of relevant shifts δ and rotations ω of the coils.

A similar procedure is employed to estimate the (m,n) error fields associated with deviations $\Delta_{k,l}(\phi_k^{'})$ in the toroidal coil system:

$$B_{m,n}^{(c,s)}(tor) = \sum_{k=1}^{18}\sum_{l=1}^{10} b_{m,n}^{(c,s)} \cdot \left[\phi_k'; \Delta_{k,l}'(\phi_k')\right] \cdot \Delta_{k,l}(\phi_k'). \tag{8.65}$$

The final form is

$$B_{m,n}^{(c,s)}(error) = B_{m,n}^{(c,s)}(tor) + B_{m,n}^{(c,s)}(pol). \tag{8.66}$$

$$B_{m,n}^{(0)} = \sqrt{\left(B_{m,n}^{(c)}\right)^2 + \left(B_{m,n}^{(s)}\right)^2},$$

$$\Psi_{m,n} = arctg(B_{m,n}^{(s)}) \,/\, B_{m,n}^{(c)}.$$

As manufacture/assembly deviations are independent and additive, it is reasonable to employ statistical methods in the analysis of error fields.

Error field modes $B_{m,n}^{(c,s)}$ are linearly dependent on shifts and tilts (rotations) of the coils or their parts. Pre-calculated error field modes $b_{m,n}^{(c,s)}(0,\delta,\omega,\Delta_\lambda)$, related to unit shifts and tilts, are the coefficients in linear combinations (8.64) and (8.65).

8.7.3 ITER Correction Coils

Despite the stringent tolerances imposed on manufacture/assembly errors of the ITER magnet system, related error fields may be two to three times higher than allowed. To suppress these errors below the LMT, a system of correction coils is provided for in the ITER design (Fig. 8.4) [11].

Eighteen superconducting correction coils are periodically distributed around the ITER and grouped in three locations: six at the top, six at the bottom, and six at mid-plane. Each pair of coils, located on opposite sides of the tokamak, is electrically connected in anti-series and magnetically coupled to provide suppression of the $n = 1$ error field modes. Each group has three independent power supplies, which allow the phase adjustment of the correcting field modes. As a result, nine independent power supplies enable reduction of three error modes to an acceptable level.

8.8 PLASMA COLUMN POSITION AND SHAPE RECONSTRUCTION BASED ON MAGNETIC MEASUREMENTS

8.8.1 Basic Principles

The position of a plasma column within the vacuum vessel is one of the main parameters controlled during a discharge. Its reliable and fast identification is

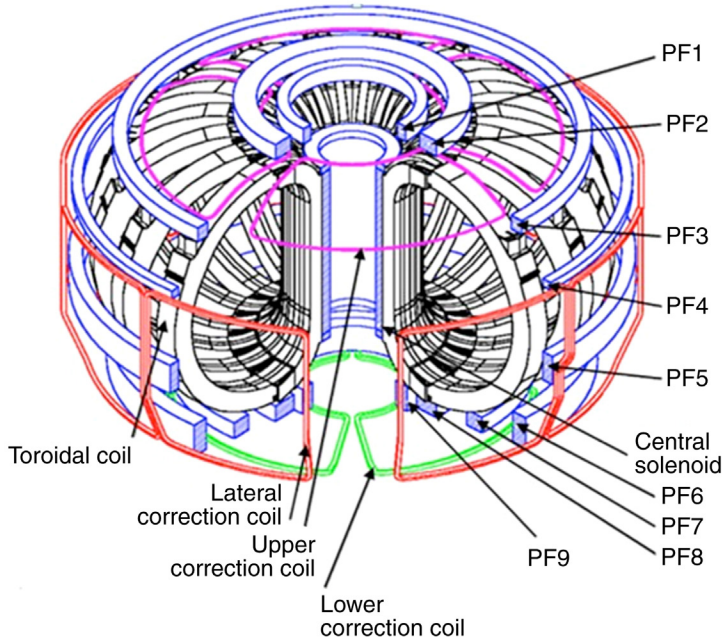

FIGURE 8.4 Arrangement of ITER correction coils. (Copyright ITER Organisation, 2017).

particularly important for tokamaks, in which equilibrium is provided by the feedback control of plasma displacements. Relevant methods rely on the measurement of poloidal magnetic fields outside the plasma using electromagnetic sensors.

The development of diagnostic systems based on magnetic measurements involves a number of fundamental issues that have to be addressed. First, the sensors must be adapted to the design and operation environment. Second, algorithms must be developed for the reconstruction of the spatial position and shape of a magnetic flux surface regarded as a plasma boundary. The precision and speed requirements for such algorithms depend on their application (information systems, closed-loop control systems, etc.) and on plasma itself, that is, on the time of the plasma parameter changes.

In ITER and tokamak-based neutron sources, the installation of sensors nearby plasma is a much more difficult task than in experimental tokamaks. The sensors are exposed, among other things, to an intense neutron radiation. This places additional constraints on the sensors number, position and design, and requires radiation effects to be taken into account. Also, plasma reconstruction algorithms must be verified as fitting for reactor-relevant conditions. In

the early days of plasma experiments, methods based on the theory of toroidal plasma turn in an external magnetic field gained. Minimum amount of measurements was ensured by the use of a sector loop or a toroidal loop for measuring the magnetic flux through the plasma cross-section, the Rogowski coil kits for measuring the discharge current and a couple of magnetic probes for measuring the tangential component of the poloidal field (the T-3 and TFR-600 tokamaks). The CLEO and TFTR tokamaks employ cosine-winding and sine-winding Rogowski coils (to indicate the column radial and vertical movements, respectively) instead of the magnetic probes.

Most of the magnetic diagnostic methods developed for tokamaks are based on the Grad–Shafranov equation, a framework that allowed, for example, integral equations for the toroidal current density momenta to be derived. The respective method relies on a comprehensive measurement of the poloidal field distribution over a selected contour around the plasma. To use this method, one needs a large number of probes detecting the normal and tangential components of the magnetic field. The main problem with this method is the complexity of the computational algorithm and the need for high-performance interference-protected probes.

At a later stage of fusion research, a range of magnetic diagnostics methods were mathematically formalised and implemented with the aid of computational codes. Since then, the development vector is towards the improvement of computational precision and speed. In present-day tokamaks, the full reconstruction of the equilibrium has normally been performed off-line using a computation-intensive fitting code such as EFIT based on a least-squares fit of the diagnostic data to the Grad–Shafranov model [12]. The small modifications to the EFIT reconstruction algorithm allowed using that algorithm in real-time execution with appropriate digital computing technology, and the results are practically identical to a standard equilibrium reconstruction technique [13].

Plasma magnetic diagnostics falls into the class of the so-called incorrect inverse problems of mathematical physics, characterised by a complex computation process and requiring a regularisation procedure [14]. Most of the plasma magnetic diagnostics methods are based on the a priori parametric notion of the flux function and only differing in adopted forms of this notion. The parameters of each individual notion are obtained by minimizing the difference between measured and computed values, and the set of measured parameters differs from method to method. Codes implementing the models of a continuous distribution of plasma parameters are usually most efficient, but too cumbersome and time-consuming, unfortunately. They are mostly used to analyse parameters in the pause between discharge current pulses. To promptly determine plasma parameters, first of all the plasma position and shape, one needs a simplified and verified phenomenological model and relevant measurement techniques.

Simple models are especially fitting for controlling a discharge in real time, when computation speed becomes a limiting factor and should be within a few milliseconds.

The present-day methods of plasma column reconstruction based on magnetic measurements and fitting for controlling the plasma in real time are classified as follows [14]:

- *The harmonic method* that relies on the flux function decomposition (usually in terms of toroidal geometry) in series using eigenfunctions of the Grad–Shafranov differential operator. The parameters to be determined are the radius of the toroidal coordinate system base circle and coefficients for the first and a few subsequent harmonics.
- *The local approximation method*, based on expressing plasma in terms of a flux function in the form of a Taylor series in the vicinity of several characteristic plasma points. In other words, it focuses on plasma points most important for control purposes, instead of the whole plasma boundary. The parameters to be determined are the Taylor series coefficients.
- *The simple-layer potential method*, involving the plasma column substitution with some closed virtual surface located inside the column and not necessarily coinciding with its boundary. The whole of the plasma current is taken to be distributed on this surface. The position of the surface depends upon parameters to be determined.
- *The current filament method*, based on approximation of the discharge current by a number of current filaments. Within this approach, one can distinguish two modifications that differ in the set of parameters to be reconstructed. In the modification of fixed current filaments, one needs to determine only the magnitudes of the filament currents, whereas the location of the current filaments is fixed. In the modification of movable current filaments, it is necessary to determine the current magnitudes and the coordinates of the current filaments.

8.8.2 Reconstruction Methods

The local approximation and current filament methods are often used for the solution of the reconstruction problem because they allow quick identification of plasma position and shape due to algorithm simplicity.

The local approximation method seeks to determine the coordinates of characteristic (special) points on the plasma column boundary that are important for plasma performance and should be controlled. For a divertor plasma configuration, the following algorithm is used. Near each special point a region is isolated, where magnetic field sensors are located. Every such region must have a toroidal loop. Numerical simulation is used for each region to determine

the best point where the flux function Ψ can be decomposed in series using basis functions. The toroidal loops are located in these points. The flux function value, $\Psi = \Psi(x)$, is calculated for the *X*-point whose coordinates are found in the divertor region. The coordinates of other special points are calculated from $\Psi = \Psi(x)$.

The movable current filament method is based on a model that assumes that the plasma current is a discrete set of *N* current filaments distributed inside the plasma, so that

$$j_\varphi(r,z) = \sum_{j=1}^{N} \delta(r - r_j, z - z_j) I_j, \tag{8.67}$$

where r_j, z_j and I_j are the coordinates and the current of the j^{th} filament, and $\delta(r - r_j, z - z_j)$ is the Dirac delta function. In a general case, system (8.67) has $3N$ free parameters: $2N$ coordinates and N currents. Its advantage is that it allows any magnetic magnitude $y(r,z)$ (flux, field and current momenta) to be computed using a Green's function Q for current filaments, which is known:

$$y(r,z) = \sum_{j=1}^{N} Q(r,z,r_j,z_j) I_j. \tag{8.68}$$

The model underlying this method has fixed currents in all filaments, while the filament coordinates are unknowns. These coordinates are found by the best agreement between the Eq. (8.68) calculations and magnetic signals measured with the sensors:

$$y \quad (r_i, z_i, r_j, z_j) = \overline{y} \quad (r_i, z_i), \quad i = 1,...,M, \tag{8.69}$$

where M is the number of measurements that must be equal to or exceed $2N$. The (8.69) non-linear system is solved using Newton's iterative method:

$$r_j^{k+1} = r_j^k + \Delta r_j^k, z_j^{k+1} = z_j^k + \Delta z_j^k,$$

$$\sum_{j=1}^{N} \frac{\partial Q_{ij}^k}{\partial r_j} I_j \Delta r_j^k + \frac{\partial Q_{ij}^k}{\partial z_j} I_j \Delta z_j^k = \overline{y}_i - y_i, i = 1,...,M. \tag{8.70}$$

The problem is considered to be solved if increments Δr, and Δz become smaller than the given small value.

Two points that remain theoretically unclear in the solution of the system of nonlinear equations by iterative methods are the computational convergence

condition and the initial approximation effect. In our case, the convergence is achieved if filaments inside the plasma instead of those nearby the magnetic field sensors are referred to as an initial approximation.

The method of movable current filaments is universal with respect to type of sensors and their locations.

The fixed current filament method is also based on a model of thin current filaments. The filament coordinates are specified, and the current amplitudes are derived by the best agreement between the calculated (y_j) and measured ($\overline{y}$) components of the poloidal magnetic field or measured flux in places where sensors and loops are located ($r_j, z_j; j = 1,..., M$). This condition is identical to the minimum of functional

$$J = \sum_{i=1}^{M} \frac{\left(y_i - \overline{y}_i\right)^2}{\sigma_i^2}, \tag{8.71}$$

where M is the number of measurements, and σ_i is the i^{th} measurement's standard deviation. The optimum locations and number of current filaments are selected by the fixed current filament method, provided that the deviation of the reconstructed boundary by the current filaments from some basic boundary with a known shape is minimal.

A comprehensive comparison of these methods suggests that the technique best fitted to the plasma control at every stage of the discharge is the movable current filament method.

REFERENCES

[1] A. Portone, Perturbed solutions of fixed boundary MHD equilibria, Nucl Fusion 44 (2004) 265.

[2] V. Belyakov, A. Kavin, Derivation of the linear models for the analysis of the plasma current, position and shape control system in tokamak devices, in: Proceedings of the International Conference 'Physics and Control' St. Petersburg, Russia, 2003. pp. 1019–1024.

[3] R.R. Khayrutdinov, V.E. Lukash, Studies of plasma equilibrium and transport in a tokamak fusion device with the inverse-variable technique, J. Comp. Phys. 107 (2) (1993) 106.

[4] V. Lukash, Y. Gribov, A. Kavin, R. Khayrutdinov, M. Cavinato, Simulations of ITER scenarios, Plasma Devices Oper. 13 (2) (2005) 143–156 (June).

[5] D.A. Ovsyannikov, E.I. Veremey, A.P. Zhabko, V.A. Belyakov, A.A. Kavin, in: Proc. of 3rd International Workshop 'Beam Dynamics & Optimization' (BDO-96), St. Petersburg, Russia,1996 1–5 July. pp. 218–229.

[6] J.C. Doyle, B.A. Francis, A.R. Tannenbaum, Feedback Control Theory, MacMillan Publ. Co, New York; Toronto, (1992) pp. 1–227.

[7] B. Lloyd, P.G. Carolan, C.D. Warrick, ECRH-assisted start-up in ITER, Plasma Phys. Controlled Fusion 38 (1996) 1627.

[8] V.A. Belyakov, A.A. Kavin, S.A. Lepikhov, A.B. Mineev, A.D. Ovsyannikov, Токамак: Начальная Стадия Разряда (Tokamak: The Initial Stage of a Discharge), Lan' Publishing House, Saint Petersburg, Russia, (2014) pp. 1–176. (www.e.lanbook.com).

[9] Y. Gribov, V. Amoskov, E. Lamzin, N. Maximenkova, E. Lamzin, J.E. Menard, J.-K. Park, V. Belyakov, J. Knaster, S. Sytchevsky, et al. Error Fields Expected in ITER and their Correction, 24th IAEA Fusion Energy Conference (2012) San Diego, USA, Paper ITR/P5-29.
[10] V. Amoskov, A. Belov, V. Belyakov, O. Filatov, Yu. Gribov, E. Lamzin, et al. Fourier analysis of 3D error fields in tokamaks, Plasma Devices Oper. 12 (2004) 285.
[11] R.J. Buttery, A.H. Boozer, Y.Q. Liu, J.-K. Park, N.M. Ferraro, V. Amoskov, et al. The limits and challenges of error field correction for ITER, Phys. Plasmas 19 (2012) 056111.
[12] L.L. Lao, et al. Nucl. Fusion 25 (1985) 1611.
[13] Ferron, J.R., et al. Real Time Equilibrium Reconstruction for Tokamak Discharge Control, General Atomics Report, GA-A22586 (1997).
[14] V.M. Amoskov, et al. Real-time determination of the position and shape of the plasma column from external magnetic measurements in the GLOBUS-M tokamak, Plasma Phys. Rep. 29 (12) (2003) 997–1008.